# MULTI-HOP COVERAGE EXTENSION OF AN IEEE 802.11B WLAN IN A CORPORATE ENVIRONMENT

*V. Capdevielle*, T. Lestable*⋆, M. Coupechoux*⋄, M.-L. Alberi-Morel*, and L. Brignol**

* Alcatel Research and Innovation, Marcoussis, France
⋆ Supélec, Gif-sur-Yvette, France
⋄ Institut Eurecom, Mobile Communications Group, Sophia-Antipolis, France.
marceau.coupechoux@alcatel.fr

## ABSTRACT

In this paper, we propose to extend the coverage of IEEE 802.11b cells in indoor environments thanks to the multi-hop concept. By adding some relay nodes to the cell, that do not need to be connected to the wired network, it is shown that we can overcome the rapidly decreasing signal strength in an office environment, reduce the number of dead spots, and so drastically reduce the number of access points per unit area. Monte Carlo simulation results are provided for a practical corporate environment. In the presented scenario, the expected covered area is tripled thanks to relay nodes. Simulations also show a cellular capacity increase (CCI) thanks to link adaptation (LA) exceeding 6. A general method for the computation of the carrier to interference ratio (CIR) in a multi-hop cloud is presented. A modelization of the joint probability density function (pdf) related to the received power and the CIRs for each physical (PHY) modes is also proposed.

## 1. INTRODUCTION

Recent years have seen a growing interest of the research community for multi-hop networks. Such packet networks can be a low cost and easily deployable technology to provide Internet access in a wireless environment and to complement the coverage of future cellular networks.

In third generation cellular networks, an example of multi-hop concept for coverage extension is given by "opportunity-driven multiple access (ODMA)", which is an option for extended coverage of UTRA TDD. [1, 2] show that ODMA provides a capacity improvement in many cases over the non-relaying system, especially when the intra-cell traffic is significant.

The project SOPRANO [3] focuses also on overlaying multi-hop networks on a cellular structure. In this context, [4] provides a closed-form formula for the probability density function of power and interference at each receiver. [5, 6] give an upper limit for interference and shows that for the same cell size and power consumption, the network with relays can significantly increase the system capacity.

In this paper, we address the issue of deep indoor coverage by the IEEE 802.11b wireless LAN (WLAN) technology [7, 8]. This standard offers data rates up to 11 Mbps and represents a very fast growing market. However, office and semi-office, where WLAN are likely to be deployed, are very challenging propagation environments, that reduce the cell coverage with respect to the free space case and create dead zones in buildings.

In order to overcome this problem, we propose to deploy very flexible and low cost relays, able to route the traffic from mobile nodes to the access point (AP) and vice versa. Section 2 provides the simulation model. For the computation of CIR in a multi-hop cloud, a general method is presented. A modelization of the joint pdf related to both the received power and the CIRs for each PHY mode is also proposed. Section 3 gives simulation results and section 4 concludes the paper.

## 2. MODELIZATION

A multi-hop cloud consists in an AP that is a gateway to the wired network, one or several relays that belong to the network architecture, and mobile stations (MS) allowed to move inside the room covered by the AP and the relays.

It is assumed that the routing protocol has found a unique route from the considered MS to the AP and that this route is the same from the AP to the MS. Moreover, we assume that the routing protocol randomly chooses one of the shortest paths. In simulations, this path is computed using the Dijkstra algorithm.

### 2.1. Monte Carlo Simulations

Coverage prediction (carrier C and CIR) results from link budget calculations over a high number of iterations. Each iteration represents a photography of the observed area. Interfering MS positions, shadowing, and communication direction are randomly selected from one snapshot to another. At each iteration, C and CIR are computed on a grid of MS receivers in the analyzed area.

The area is characterized by an indoor propagation environment delimited by the walls of buildings and an outdoor zone. Details for the propagation model are given in section 2.3.

The power received by the considered MS comes from a selected relay (or AP). It is the last node on the route towards the AP. Interference is the received power resulting from the other simultaneous transmissions in the cloud. The process for selecting the interfering active nodes is deeply described in the following section.

### 2.2. Computation of C and CIR

The goal of this section is to compute C and CIR inside a multi-hop cloud at a given receiver point, which in communication over the flow $F^*$. The network is represented by a graph $G = (V, E)$ (see example on Fig.1). The edges are the AP, the relays, and the MSs. If $u$ and $v$ belongs to $E$, the vertice or flow $(u, v)$ belongs to $V$ iff a communication between $u$ and $v$ is possible at a predefined basic rate. The predefined basic rate is the rate at which RTS/CTS packets are sent, i.e., 1 or 2 Mbps. A communication is possible iff at the basic rate, the mean packet error rate (PER) remains below a PER target (PERT):

$$\begin{aligned} \forall(u,v) \in E^2, (u,v) &\in V \iff \\ E[PER(Basic\ Rate)] &\leq PERT\ . \end{aligned} \tag{1}$$

For the computation of $C$ at a given receiver point, a definition of the uplink and the downlink is needed in the multi-hop cloud. The uplink communication is the communication between the MS and the next node on the route towards the AP. The downlink is the reverse link. Let's denote R(MS) the last node on the route from the AP to the MS (cf. routing rule assumed above). $C$ is the received power at MS (for the downlink) or R(MS) (for the uplink).

For the computation of $I$, a set, $\Theta$, of flows that take advantage of spatial reuse in the multi-hop cloud to transmit simultaneously with the considered flow $F^*$ has to be determined. Note that inside a cloud, all nodes share the same frequency channel. Then, following [5], the model for channel interference is to sum the interference powers and treating the total as Gaussian noise. The main idea of the proposed algorithm is to randomly extract a clique from the flow graph and add all transmitted powers at the receiver.

When a flow $F$ has won the channel thanks to the exchange of RTS/CTS control packets, all flows in a distance of two hops from $F$ are not allowed to transmit, because involved pairs have heard RTS and/or CTS and prevent themselves to send data packets. Let us denote $H_2(F)$ the set of flows that are two hops away from $F$.

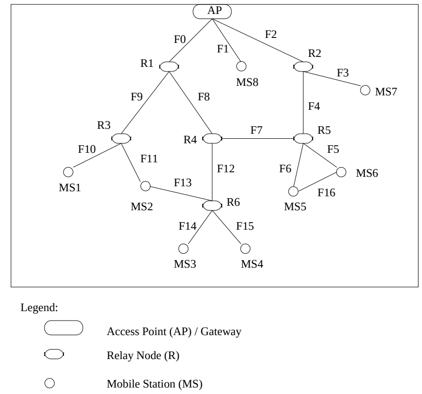


**Fig. 1**. Example of multi-hop cloud with an AP, 6 relays, and 8 MS.

As an example, the downlink flow $F_{14}$ (see Fig.1) is considered. $R_6$ has sent a RTS that has been received by $MS_2$, $MS_4$, and $R_4$. All these nodes prevent themselves to get involved in another communication beause of the virtual carrier sensing. Hence, $H_2(F_{14}) = \{F_{15}, F_{13}, F_{12}, F_{11}, F_7, F_8\}$.

Now, $H_2(F)$ can be seen as the set of contending flows for $F$. If we assume that the MAC protocol is fair, the probability for $F$ to access the channel should be proportional to $1/d(F)$, where $d(F) = Card(H_2(F))$ is the cardinal of $H_2(F)$, e.g., $d(F_{14}) = 6$. This result is in compliance with the main result of [9] that claims that the maximum probability of a successful transmission is upper bounded by $0.9278$ $/N$, where $N$ is the average number of nodes within a transmission range.

These considerations lead to the following algorithm for $F^*$. Direct communications between MS may not be allowed. In this case, the corresponding flows, e.g., $F_{16}$, are not considered as contenders for the shared medium.

1. $\Theta = \{F^*\},\ T = E \setminus \{\{F^*\} \cup \{F_i | F_i$ not allowed$\}\}$.
2. For each $F$ in $V$, build $H_2(F)$ and compute $d(F) = Card(H_2(F))$.
3. $T = T \setminus \{H_2(F^*)\}$.
4. While $T \neq \oslash$,
   (a) Choose randomly $F_i$ in $T$ with probability $\alpha/d(F_i)$, $\alpha$ is such that $\alpha \sum 1/d(F_i) = 1$.
   (b) $\Theta = \Theta \cup \{F_i\}$.
   (c) $T = T \setminus \{F_i\}$.
   (d) $T = T \setminus \{H_2(F_i)\}$.
5. For each $F$ in $\Theta$, $F$ is considered to be uplink with probability $p_{UL}$, otherwise it is a downlink.
6. $I$ is the aggregate received power from all flows $F$ in $\Theta$.

### 2.3. Path Loss Model in Mixed (outdoor-indoor) Environments

The path loss model is supposed to be a log-distance model for the outdoor path to which an extra loss due to the external wall attenuation and to the indoor propagation is added. The resulting model is continuous and describes the propagation in a mixed environment.

$$\begin{aligned} L(f) &= a(f) + 20\log(1 + d_{out}/d_{in}) \\ &\quad + \underbrace{20\log(d_{in}) + \alpha d_{in} + Wall}_{\text{indoor attenuation}} \qquad (2) \\ a(f) &= 32.4 + 20\log(f), \qquad (3) \end{aligned}$$

where $f$ is the carrier frequency ($2.412$ GHz), $d_{out}$ and $d_{in}$ are the total outdoor and indoor distances, $\alpha$ is a constant used to model propagtion in an homogeneous indoor environment, and $Wall$ is an additive constant which takes into account the attenuation by an external wall. The received power is computed from link budget calculations with an additive log-normal distribution modeling shadowing.

### 2.4. Link Adaptation

The policy of link adaptation employed in our scheme is based on PER metric and CIR switching thresholds. That means that PHY modes are chosen due to both C (sensitivity imposed by the standard) and CIR measurements (with PER constraint). This strategy has lead to the definition of the following CIR thresholds (in dB): $[0\ 3.8\ 5.7\ 6.7]$, that corresponds respectively to PHY modes $1$, $2$, $5.5$, and $11$ dB.

### 2.5. Scenario Description

For our simulations, one of the buildings of the Alcatel Research Center in Marcoussis (France) has been considered (see Fig.2). This building is approximatley $50$m and $150$m long. 20 nodes are assumed to be active. The AP and the four relays form a string topology. Other simulations parameters are shown in Tab.1.

It is clear that the AP location is not an optimal choice. It has been deliberately placed at the extremity of the building to show that deep indoor coverage is possible with relay nodes.

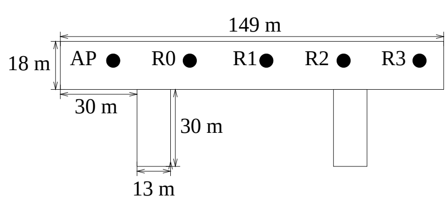


**Fig. 2**. Analyzed building.

**Table 1**. Simulation Parameters

| Parameter | Value |
|---|---|
| AP, relay, MS transmit power | $15$dBm |
| Transmit antenna gains | $0$dBi |
| Receive antenna gain | $0$dBi |
| Receiver sensitivity threshold | $-94$dBm |
| Shadowing standard deviation | $4$dB |
| Thermal noise power | $-101$dBm |
| Uplink traffic load | $30\%$ |
| Downlink traffic load | $70\%$ |
| Number of MS | $20$ |

## 3. SIMULATION RESULTS

### 3.1. Performance Metrics

Two metrics are introduced. The first one is a measure of the coverage gain thanks to the deployement of relay nodes. The reduction of non covered area (RNC) is the proportion of non covered area with an AP alone that is now covered thanks to the relay nodes:

$$RNC = (\%NC - \%NCR)/\%NC, \qquad (4)$$

where $\%NC$ is the proportion of indoor area non covered by the AP alone and $\%NCR$ is the proportion of indoor area not covered by the AP with the relays. Note that $RNC = 1$, when the whole indoor area is covered.

The second metric refers to the capacity gain obtained with link adaptation [10]. This is the cellular capacity increase (CCI):

$$CCI = E[TLA]/E[T], \qquad (5)$$

where $E[TLA]$ and $E[T]$ are the average surfacic throughputs resp. with and without link adaptation.

### 3.2. Coverage Extension

In this section, we compare the percentage of not covered areas if relays are used or not. The software provides coverage maps (C or CIR) resulting from the statistical average of the computations per snapshot. By applying the link adaptation mechanism to those average values, they are converted in expectable PHY modes.

By comparing the PHY modes maps (Fig.3 and Fig.4 are an example of snapshot) resulting from the two cases, AP alone and AP with relays, the RNC brought by the added relays is computed. In this example, $RNC = 0.95$. Moreover the indoor covered area is tripled. This result must be counter balanced by the fact that the user throughput is reduced when multiple hops are needed to reach the MS (downlink) or the AP (uplink). However, the cost of installation is

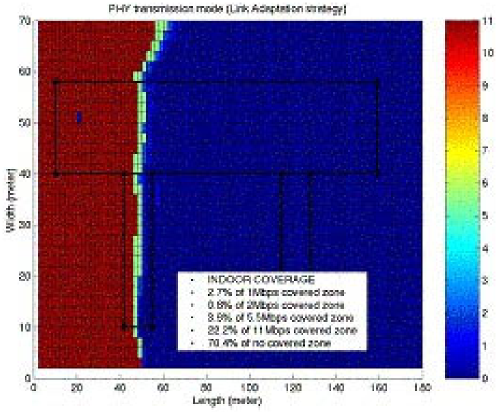


**Fig. 3**. PHY modes map, 1 AP without relay nodes.

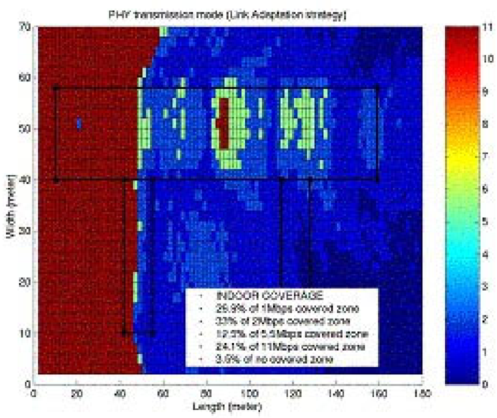


**Fig. 4**. PHY modes map, 1 AP and 4 relay nodes.

reduced because relays do not need to be connected to the wired network and the deployement is very flexible.

Not that high PHY modes are not present around the relay nodes. This phenomenon can be explained by the assumed routing algorithm that chooses routes with the minimum number of hops. Indeed, a MS close to the first relay is still in the communication range of the AP, and so will preferably be attached to the AP with a low PHY mode, rather than to the relay with a high PHY mode.

### 3.3. CIR Distribution and Cellular Capacity Increase

The estimated CCI is computed thanks to Eq.5. Throughputs are averaged over all positions of the analyzed grid and all iterations of the Monte Carlo simulation. On this example, $CCI = 6.4$.

In order to study the impact of the link adaptation on the cell capacity, an analytical modelling has been tackled. The first issue is to efficiently model the joint pdf related to both received powers C (see Fig.5), and CIRs for each PHY mode (Fig.6). These pdf are approximated by generalized gamma distributions with parameters $(\alpha_C, \beta_C)$ (for C), $(\alpha_1, \beta_1)$ (for $R_1$ = 1Mbps), $(\alpha_2, \beta_2)$ (for $R_2$ = 2Mbps), $(\alpha_3, \beta_3)$ (for $R_3$ = 5.5Mbps), and $(\alpha_4, \beta_4)$ (for $R_4$ = 11Mbps). If $(\psi_k)_{k=1\ldots4}$ represent the occupancy probabilities of the PHY modes $(R_k)_{k=1\ldots4}$, Eq.5 can be written:

$$CCI = \frac{\sum_{k=1}^{4} R_k \psi_k}{R_1}. \tag{6}$$

The parameters of the generalized gamma distributions are obtained thanks to the least square method:

$$\alpha_C = 1.93, \qquad \beta_C = 6.70, \tag{7}$$
$$\alpha_1 = 1.30, \qquad \beta_1 = 8.25, \tag{8}$$
$$\alpha_2 = 1.55, \qquad \beta_2 = 7.40, \tag{9}$$
$$\alpha_3 = 2.82, \qquad \beta_3 = 4.90, \tag{10}$$
$$\alpha_4 = 4.65, \qquad \beta_4 = 3.59. \tag{11}$$

The explicit computation of the $(\psi_k)_{k=1\ldots4}$ is explained in appendix. Finally, analytical results give a CCI equal to $6.39$ which is a good approximation of the value obtained by simulations. This result also validates the proposed approach. This framework allows also the study of the impact of different CIR thresholds on the CCI.

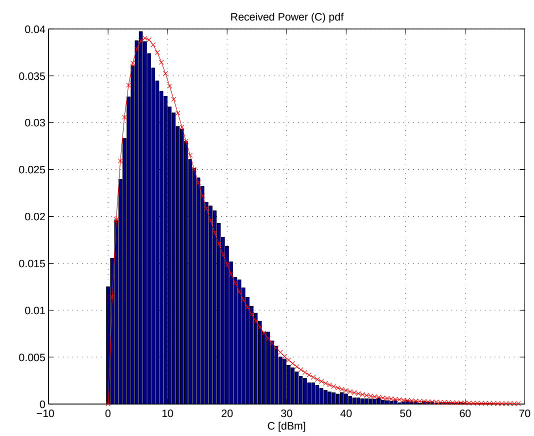


**Fig. 5**. Probability density function of C and approximation by a generalized gamma distribution.

## 4. CONCLUSION

In this paper, a coverage extension of an IEEE 802.11b cell in an indoor environment has been proposed. This extension uses relay nodes able to route information from and to an AP in a multi-hop fashion. Monte Carlo simulations prove the

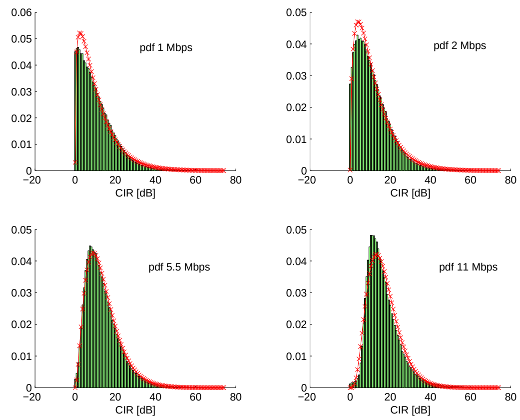


**Fig. 6**. Probability density functions of CIR and approximations by generalized gamma distributions.

benefit of such a solution in the practical case of a corporate building: deep indoor coverage is possible thanks to low cost and easily deployable relay nodes. This gain is obtained at the cost of a user throughput degradation due to the multiple hops. At last, an analytical modelization based on these results shows the cellular capacity increase induced by link adaptation.

### 5. REFERENCES


[1] T. Rouse, S. McLaughlin, and H. Haas, "Coverage-capacity analysis of opportunity driven multiple access (odma) in utra-tdd," in *Proc. of IEE 3G Mobile Communication Technologies*, 2001.

[2] T. Rouse, I. Band, and S. McLaughlin, "Capacity and power investigation of opportunity driven multiple access (odma) networks in tdd-cdma based systems," in *Proc. of IEEE ICC*, 2002.

[3] N. Zadeh, B. Jabbari, R. Pickholz, and B. Vojcic, "Self-organizing packet radio ad hoc networks with overlay (soprano)," *IEEE Communication Magazine*, June 2002.

[4] N. Zadeh and B. Jabbari, "Performance analysis of multihop packet cdma cellular networks," in *Proc. of IEEE GLOBECOM*, 2001.

[5] N. Zadeh and B. Jabbari, "Throughput of a multihop packet cdma network with power control," in *Proc. of IEEE VTC Spring*, 2000.

[6] N. Zadeh and B. Jabbari, "On the capacity modeling of multihop cellular packet cdma cellular networks," in *Proc. of IEEE MILCOM*, 2001.

[7] 1999 Edition ANSI/IEEE std. 802.11, "Part11: Wireless lan medium access control (mac) and physical layer (phy) specifications," 1999.

[8] 1999 Edition ANSI/IEEE std. 802.11b, "Part11: Wireless lan medium access control (mac) and physical layer (phy) specifications: Higher-speed physical layer extension in the 2.4 ghz band," 1999.

[9] R. Nelson and L. Kleinrock, "Maximum probability of successful transmission in a random planar packet radio network," in *Proc. of IEEE INFOCOM*, 1983.

[10] V. Capdevielle, T. Lestable, and L. Brignol, "Cellular capacity enhancement thanks to link adaptation in hiperlan/2," in *IST Mobile Communication Summit*, 2001.


# Appendix

Let $\gamma$ be the generalized gamma distribution used to approximate the considered pdf.

$$\gamma(x|\alpha,\beta) = \frac{\beta^{\alpha}}{\Gamma(\alpha)} x^{\alpha-1} e^{-\beta x}. \tag{12}$$

Then, let us define the complementary incomplete gamma function:

$$Q(a,x) = \frac{1}{\Gamma(a)} \int_{x}^{+\infty} t^{a-1} e^{-t} dt, \tag{13}$$

with $Q(a,0) = 1$ and $Q(a,+\infty) = 1$. Now, the probability to have a 11 Mbps PHY mode is the probability that C is over the sensitivity threshold defined by the standard for 11 Mbps, $S_4$, and that the CIR is over the CIR threshold provided by the link adaptation strategy, $\gamma_4$, given that the point is covered. This can be written:

$$\begin{aligned} \psi_4 &= \frac{P[C > S_4, \gamma > \gamma_4]}{P[C > S_1]} && (14)\\ &= \frac{P[C > S_4]P[\gamma > \gamma_4 | C > S_4]}{P[C > S_1]} && (15)\\ &= \frac{Q(\alpha_C, \beta_C S_4) Q(\alpha_4, \beta_4 \gamma_4)}{Q(\alpha_C, \beta_C S_1)}. && (16) \end{aligned}$$

With similar arguments, it is straightforward to deduce the other probabilities of occupancy.

$$\begin{aligned} \psi_2 &= \frac{Q(\alpha_C, \beta_C S_2) Q(\alpha_2, \beta_2 \gamma_2)}{Q(\alpha_C, \beta_C S_1} - \\ &\quad \frac{Q(\alpha_C, \beta_C S_3) Q(\alpha_3, \beta_3 \gamma_3)}{Q(\alpha_C, \beta_C S_1)} && (17)\\ \psi_3 &= \frac{Q(\alpha_C, \beta_C S_3) Q(\alpha_3, \beta_3 \gamma_3)}{Q(\alpha_C, \beta_C S_1)} - \\ &\quad \frac{Q(\alpha_C, \beta_C S_4) Q(\alpha_4, \beta_4 \gamma_4)}{Q(\alpha_C, \beta_C S_1)} && (18) \end{aligned}$$